Configuration and Internal Dynamics of $CH_2ClF\cdots$Krypton†

Paolo Ottaviani,‡ Biagio Velino,§ and Walther Caminati*,‡

Dipartimento di Chimica "G. Ciamician" dell'Università, Via Selmi 2, I-40126 Bologna, Italy, and Dipartimento di Chimica Fisica e Inorganica dell'Università, Viale Risorgimento 4, I-40136 Bologna, Italy

Received: July 16, 2007; In Final Form: August 18, 2007

The molecular complex chlorofluoromethane−krypton has been investigated by Fourier transform microwave spectroscopy in a supersonic expansion. The rotational spectra have been assigned for the $CH_2{}^{35}ClF\cdots{}^{84}Kr$, $CH_2{}^{35}ClF\cdots{}^{86}Kr$, and $CH_2{}^{37}ClF\cdots{}^{84}Kr$ species, showing that, in the equilibrium configuration, the krypton atom is located out of the ClCF plane, interacting with both F and Cl atoms. All rotational transitions are split in several ^{35}Cl or ^{37}Cl quadrupole components, each of them further split into two lines, due to the tunneling motion of the Kr atom between two equivalent positions, below and above the ClCF plane. The feasible low-energy pathway between these two structurally degenerate conformations is described, in a first approximation, by a circular motion around the C−Cl bond, with a barrier estimated to be about 74 cm^{-1}.

Introduction

Dispersion forces are the basis for the stability of molecular complexes of rare gases and thus the investigations of these adducts allow us to characterize such interactions. Several rotational spectra of molecular adducts of krypton with organic molecules have been investigated.[1−9] Their features change dramatically in going from complexes with cyclic (mainly aromatic) molecules to complexes with open chain molecules. In the first case, the Kr atom is relatively firmly located on one side of the plane and does not produce vibrational tunneling and consequent splittings on the rotational transitions.[1−5] Vice versa, the complexes with small noncyclic organic molecules, such as dimethyl ether−Kr,[7] acetaldheyde−Kr,[8] and difluoromethane−Kr,[9] display doublings of the rotational transitions, which allows for the evaluation of the potential energy surface of the tunneling motions.

Adducts of Freon-31, chlorofluoromethane (CH_2ClF), with water[10] and Ar[11] have recently been characterized by rotational spectroscopy. Both spectra showed splittings of the rotational transitions due to the water and argon motions. In the case of $CH_2ClF\cdots$water, the splittings are originated by the internal rotation of water around its C_{2v} symmetry axis.[10] In the case of $CH_2ClF\cdots$Ar,[11] the doubling is due, in a first approximation, to a rotation of the Ar atom around the C−Cl bond. This motion was quite different with respect to the model proposed for difluoromethane−Ar[12] and difluoromethane−Kr,[9] when the rare gas (Rg) atom was tunneling from above to below the FCF plane through a pathway in between the two fluorine atoms and in the plane HCH.

We considered it interesting to investigate how the replacement of the Rg atom (heavier than Ar) would affect the potential energy surface of the $CH_2FCl\cdots$Rg series. For this reason, after $CH_2FCl\cdots$Ar, we decided to investigate the rotational spectrum of $CH_2ClF\cdots$Kr. In contrast to Ar, Kr possesses isotopes in large natural concentration, whose rotational spectra allow for a better location of the noble gas atom in the complex. A sketch of $CH_2ClF\cdots$Kr is given in Figure 1. The principal axis systems of CH_2ClF and the polar coordinates required for the distributed polarizability model calculations (presented in one of the next sections) are indicated.

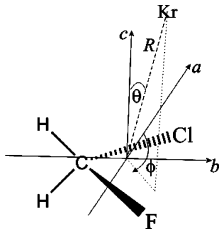

Figure 1. Sketch of $CH_2ClF\cdots$Kr with the definition of the coordinates used in the DPM model calculations.

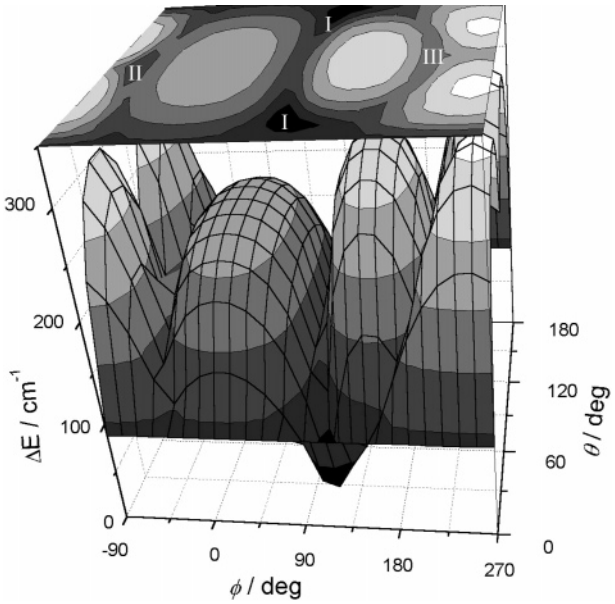

Figure 2. Potential energy surface of $CH_2ClF\cdots$Kr calculated with the DPM model; grid: $\Delta\theta = \Delta\phi = 15°$.

† Part of the "Giacinto Scoles Festschrift".

* Corresponding author. E-mail: walther.caminati@unibo.it.
‡ Dipartimento di Chimica.
§ Dipartimento di Chimica Fisica e Inorganica.

10.1021/jp075552j CCC: $37.00
Published on Web 10/20/2007

TABLE 1: Spectroscopic Constants of $CH_2ClF\cdots Kr$

	$CH_2{}^{35}ClF\cdots{}^{84}Kr$		$CH_2{}^{35}ClF\cdots{}^{86}Kr$		$CH_2{}^{37}ClF\cdots{}^{84}Kr$	
	$v=0^+$	$v=0^-$	$v=0^+$	$v=0^-$	$v=0^+$	$v=0^-$
A/MHz	5450.745 (1)[a]	5450.743(1)	5450.342(3)	5450.341(3)	5345.495(3)	5345.478(3)
B/MHz	952.5186(2)	952.5174(2)	942.9543(8)	942.9542(8)	935.2976(8)	935.2969(8)
C/MHz	833.9129(4)	833.9138(4)	826.569(3)	826.568(3)	818.247(1)	818.248(1)
D_J/kHz	3.039(3)		2.92 (2)		3.039[b]	
D_{JK}/kHz	45.85(3)		45.4(1)		45.86[b]	
D_K/kHz	12.7(2)		13.1(6)		12.7[b]	
d_1/kHz	0.421(2)		0.419[b]		0.420[b]	
d_2/kHz	0.101(2)		0.101[b]		0.101[b]	
$^3/_2\chi_{aa}$/MHz	54.637(5)	54.642(5)	54.67(1)	54.68(1)	42.83(1)	
$^1/_4(\chi_{bb}-\chi_{cc})$/MHz	−16.823(2)	−16.823(2)	−16.823(3)	−16.821(3)	−13.299(4)	−13.301(4)
χ_{ab}/MHz	−11.1(3)		−10.8(5)		−11.1[b]	
$\chi_{bc-0^+0^-}$/MHz	38.46(3)		38.71(8)		29.7(1)	
$\chi_{ac-0^+0^-}$/MHz	−4.528(1)		−3.9(1)		−4.0(1)	
$\Delta E_{0^+0^-}$/MHz	0.6298(6)		0.626(1)		0.6255(1)	
$iG_{a-0^+0^-}$/MHz	−0.021(3)		−0.021(5)		−0.021[b]	
$iG_{b-0^+0^-}$/MHz	0.43(1)		0.43(1)		0.43(1)	
N[c]	125		36		42	
σ/kHz[d]	2.0		1.1		2.1	

[a] Errors in parentheses are expressed in unit of the last digit. [b] Fixed at the value of the parent species. [c] Number of lines in the fit. [d] Standard deviation of the fit.

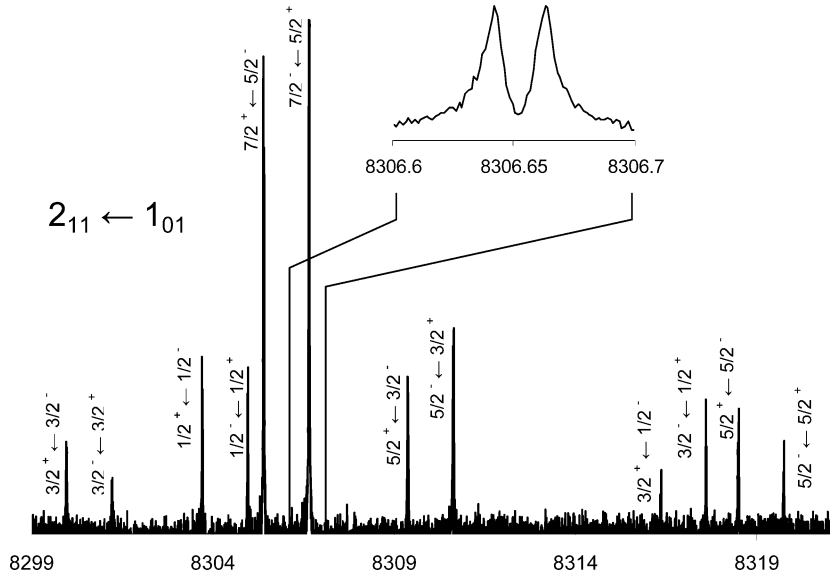

Figure 3. ^{35}Cl hyperfine structure and 0^+ and 0^- component lines of the $2_{11}-1_{01}$ μ_c transition of the observed conformer of $CH_2ClF\cdots Kr$. The Doppler doubling of each component is shown in the inset.

Experimental Methods

The rotational spectrum in the 6−18.0 GHz frequency region was measured using a COBRA-type[13] pulsed supersonic-jet Fourier transform microwave (FT-MW) spectrometer[14] described elsewhere,[15] and recently updated with the FTMW++ set of programs.[16] A mixture of 1% CH_2ClF in Kr was expanded from about 4 bar to about 10^{-5} mbar. Each rotational transition displays a Doppler splitting, originating from the expansion of the supersonic jet coaxially along the resonator axes. The rest frequency is calculated as the arithmetic mean of the frequencies of the two Doppler components. The estimated accuracy of frequency measurements is better than 3 kHz and lines separated by more than 7 kHz are resolvable with our geometry[14] when using Kr as carrier gas. CH_2ClF was supplied by Aldrich and krypton by Rivoira.

Distributed Polarizability Model Calculations of the Potential Energy Surface of $CH_2ClF\cdots Kr$

Because no complexes of Kr with a molecule containing both Cl and F atoms have been investigated before, we decided to study systematically the possible minima and barriers on the van der Waals potential energy surface with the distributed polarizability model (DPM).[17,18]

The DPM calculations were performed using the computer program RGDMIN.[19] The geometry of CH_2ClF was fixed to the experimental r_0 structure[20] whereas the distance (R_{CM}) between its center of mass (CM) and the rare gas could freely relax for energy minimization in the full range $\theta = 0-180°$, $\phi = -90$ to $+270°$ at steps of $\Delta\phi = \Delta\theta = 15°$. R_{CM}, θ, and ϕ are the spherical coordinates shown in Figure 1.

The results are quite similar to those obtained for $CH_2ClF\cdots Ar$.[11] The potential energy surface obtained is shown in Figure 2, in two- (top) and in three-dimensional ways (bottom). Four minima, labeled I (structurally doubly degenerate), II, and III, were found. Minimum type I was predicted to more stable by about 100 and 160 cm^{-1} than minima II and III, respectively. In addition, its population is favored by a statistical conformational weight 2:1. For this reason, we looked for the spectrum of species I.

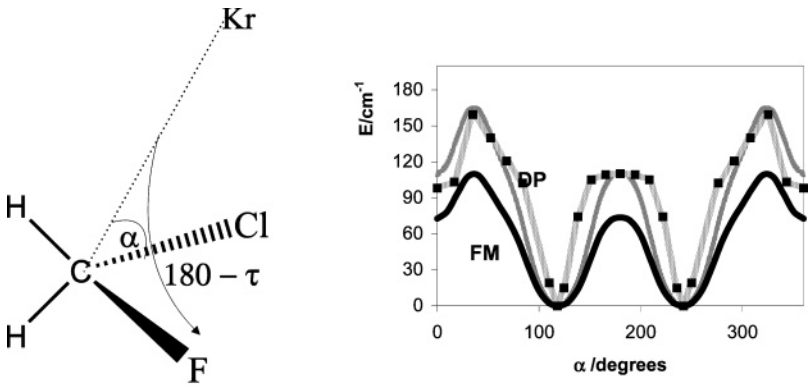

Figure 4. Left: sketch of $CH_2ClF\cdots Kr$ with the definition of the coordinates used in the flexible model calculations (R, α, and τ). Right: the lowest energy tunneling pathways as obtained by the DPM model (squares), interpolated with eq 6 (thin line), and scaled upon optimization of flexible model calculations (thick line).

Rotational Spectrum

We searched for and assigned first the spectrum of the most abundant isotopologue, $CH_2{}^{35}ClF\cdots{}^{84}Kr$ (ca. 43% in nature). Figure 3 shows its $2_{11} \leftarrow 1_{01}$ transition, which is constituted by 14 component lines: 7 ^{35}Cl quadrupole components, each of them further split into a pair of lines due to the Kr tunneling. A total of 10 μ_c-type transitions were measured. The inversion splitting was nearly constant for all of them, suggesting that the μ_c dipole moment component is inverting for the effect of the motion. Finally, it was possible to measure several weak μ_a and μ_b type transitions, some of them too split for the effects of the Kr tunneling, but with much smaller and irregular splittings. This indicates that μ_a and μ_b are not inverting for the motions of Kr.

All measured lines[21] could be fitted with a coupled two-states Hamiltonian,[22] set in the principal inertial axis system to preserve the definition of the quadrupole coupling tensor:

$$H = \sum_i (H_i^{R} + H_i^{Q}) + H^{CD} + H^{int} \qquad \text{with} \qquad i = 0, 1 \qquad (1)$$

and

$$H^{int} = \Delta E_{0^+0^-} + iG_{a-0^+0^-}\cdot\mathbf{P}_{a0^+0^-} + iG_{b-0^+0^-}\cdot\mathbf{P}_{b-0^+0^-} + H_{int}^{Q} \quad (2)$$

$$H_{int}^{Q} = [\chi_{bc-0^+0^-}(\mathbf{P}_{b0^+0^-}\mathbf{P}_{c0^+0^-} + \mathbf{P}_{c0^+0^-}\mathbf{P}_{b0^+0^-}) + \chi_{ac-0^+0^-}(\mathbf{P}_{a0^+0^-}\mathbf{P}_{c0^+0^-} + \mathbf{P}_{c0^+0^-}\mathbf{P}_{a0^+0^-})]f(I,J,F) \quad (3)$$

In eq 1 H_i^{R} and H_i^{Q} are the rigid rotor rotational and quadrupole interaction terms for the ith state, H^{CD} represents the centrifugal distortion contribution, corresponding to the I^r representation of Watson's "S" reduced Hamiltonian[23] and common to both states, and H^{int} takes into account all interactions between the two states. The last term is explicated in eq 2, with $\Delta E_{0^+0^-}$ being the energy difference between the two tunneling substates, $G_{a-0^+0^-}$ and $G_{b-0^+0^-}$ are the Coriolis coupling parameters referred to the principal axis system, and H_{int}^{Q} is the quadrupole coupling interaction term between both substates, which from symmetry reasons are associated with the off-diagonal quadrupole coupling constants $\chi_{bc-0^+0^-}$ and $\chi_{ac-0^+0^-}$ as given in eq 3. The fact that both $G_{a-0^+0^-}$ and $G_{b-0^+0^-}$ are different from zero, is consistent with a tunneling motion that generates an angular momentum with components along the a- and b-axis.

All spectroscopic constants obtained from the coupled fitting are reported in Table 1. Also the spectroscopic constants of the $CH_2{}^{35}ClF\cdots{}^{86}Kr$ and $CH_2{}^{37}ClF\cdots{}^{84}Kr$ isotopologues (ca. 13% and 14% in natural abundance, respectively) are reported here. For the assignment of the rotational spectra of these species, the same procedure described for the most abundant isotopologue was followed. However, because their spectra are weaker than that of $CH_2{}^{35}ClF\cdots{}^{84}Kr$ species, a smaller number of lines has been measured; for this reason some centrifugal distortion constants have been constrained to the corresponding value of the most abundant species. The quadrupole splittings observed for the ^{37}Cl isotopologue were smaller than those for the ^{35}Cl isotopologues, according to its smaller value of the nuclear electric quadrupole moment [$Q(^{35}Cl)$ and $Q(^{37}Cl)$ are -0.079 and -0.062 barns, respectively].

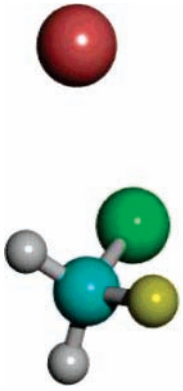

Figure 5. Observed conformer of $CH_2ClF\cdots Kr$, according to its r_0 structure.

Structure of the Complex

The r_s coordinates[24] of the krypton and chlorine atoms can be obtained in the principal axes system of $CH_2{}^{35}ClF\cdots{}^{84}Kr$ when substituting ^{84}Kr with ^{86}Kr and ^{35}Cl with ^{37}Cl, respectively. The two sets of data are shown in Table 2. The estimated errors in r_s were calculated according to Costain's formula,[25] $\delta z_i = 0.0012/|z_i|$ Å. The value of $|c|$ of the Cl atom results slightly imaginary, probably due to the Coriolis effects of large amplitude van der Waals vibrations being present in the dimer.

In Table 3 we report a partial r_0 structure of the complex, obtained fitting the distance C−Kr (R), the angle KrCCl (α) and the dihedral angle 180° − KrC−ClF (τ), shown in the left part of Figure 4. The three parameters are compared to the corresponding values obtained with the DPM calculations. The geometry of CH_2ClF has been fixed to that of the isolated molecule.[20] The complex, according to its r_0 structure, is shown in Figure 5.

TABLE 2: r_s Coordinates of Kr and Cl in the Principal Axis Systems of $CH_2ClF\cdots Kr$

	Kr		Cl	
	exptl	calc[a]	exptl	calc[a]
$\|a\|$/Å	1.651 (1)	1.658	2.222 (1)	2.206
$\|b\|$/Å	0.05 (3)	0.05	0.974 (2)	0.976
$\|c\|$/Å	0.03 (4)	0.01	0.04i (3)	0.1
r_{Kr}−Cl/Å	exptl: 3.978		calc:[a] 4.078	

[a] From the r_0 structure of Table 3.

TABLE 3: r_0 and r_{DPM} Structural van der Waals Parameters (See Text and Figure 5)

	r_0	r_{DPM}
R/Å	3.897 (2)	3.897
α/deg	83.1 (3)	79.8
τ/deg	122.7 (3)	118.0

Van der Waals Vibrations

We have already estimated the potential energy surface with the DPM model calculations. Here we check the reliability of the DPM model, by investigating how the potential energy surface obtained fit the observed tunneling splitting. Additional experimental data, such as centrifugal distortion parameters and tunneling splittings, independently supply information on the $Kr\cdots CH_2ClF$ stretching and on the tunneling motion.

(a) Van der Waals Stretching. The stretching of the Kr atom with respect to the center of mass of CH_2ClF practically takes place, as shown by the almost zero values of its $|b|$ and $|c|$ coordinates (see Table 2) along the inertial a-axis of the complex. In such a case the stretching force constant (k_s) can be estimated by considering the complex as made of two rigid parts, and using the following equation:[26−28]

$$k_s = 16\pi^4(\mu R_{CM})^2[4B^4 + 4C^4 - (B-C)^2(B+C)^2]/(hD_J) \quad (4)$$

where μ is the pseudodiatomic reduced mass, D_J is the centrifugal distortion constant and R_{CM} (3.706 Å) is the distance between the centers of mass of the monomers. The value $k_s = 2.1$ Nm^{-1} has been obtained, corresponding to a harmonic stretching fundamental $\nu_s = 31$ cm^{-1}.

By assuming a Lennard-Jones type potential the dissociation energy has been estimated by applying the approximate formula:[29]

$$E_B = (1/72)k_s R_{cm}^{\ 2} \quad (5)$$

from which a value $E_B = 2.5$ kJ/mol has been calculated.

(b) Tunneling Motion Described by One-Dimensional Flexible Model Calculations. The DPM two-dimensional potential energy surface of the angular motions of Kr around CH_2ClF is shown in Figure 2. The observed species comprises two equivalent equilibrium configurations, with tunneling splittings of 0.630, 0.626, and 0.625 MHz, for the $CH_2{}^{35}ClF\cdots{}^{84}Kr$, $CH_2{}^{35}ClF\cdots{}^{86}Kr$, and $CH_2{}^{37}ClF\cdots{}^{84}Kr$ species, respectively (see Table 1). We tried to interpret these splittings as arising from a monodimensional motion by applying a one-dimensional flexible model.[30] This model allows the numerical calculation of the rotational and vibrational wavefunctions and eigenvalues (and then the vibrational spacings) but needs a parametric description of the pathway and a potential energy function. For this purpose we individuated the DPM lower energy pathway, corresponding to the dark closed circle in the left part of the 2D graphic of Figure 2. This pathway describes a motion of Kr around the C−Cl bond and includes the two equivalent global minima represented by structure I and the point representing structure II.

To describe the angular motion of the Kr atom for the flexible model calculations, we used the coordinates R, α, and τ defined in the left part of Figure 4.

The energy profile and the structural parameters α and R as functions of τ in the flexible model calculation were taken into account using the following empirically adapted relations:

$$V(\tau)/cm^{-1} = 190\,[(\cos\tau - \cos 118.0)(1 - 0.4\cos\tau)(1 - 0.1\cos 3\tau)(1 - 0.05\cos 6\tau)]^2 \quad (6)$$

$$R(\tau)/Å = 3.897 + 0.6\,[(\cos\tau - \cos 118.0)(1 - 0.5\cos\tau)(1 - 0.1\cos 3\tau)(1 - 0.05\cos 6\tau)]^2 \quad (7)$$

$$\alpha(\tau)/deg = 68 + 8[0.2 + \cos(3\tau)][1 - 0.4\cos(2\tau)] \quad (8)$$

In eqs 6 and 7, the fist term ($\cos\tau - \cos 118.0$) locates the minima of the function, and the remaining terms fix the maxima and model the shape of the function. The experimental splittings (ca. 0.63 MHz for all isotopologues) were reproduced when scaling the potential energy function given in eq 6 by a factor 0.665, giving an effective tunneling barrier of ca. 74 cm^{-1}. $V(\tau)$ is represented in in the right part of Figure 4, where the dots represent the DPM low-energy pathway, the dashed line is the function that best fits the theoretical DPM values, and the continuous line is the scaled potential function that reproduces the experimental vibrational splitting. As seen there, minimum II would be accessible through a barrier of about 115 cm^{-1}. In the flexible model calculations the coordinate τ was considered in the full cyclic range, resolved in 87 mesh points.[30]

Conclusions

The rotational spectra of three isotopologues ($CH_2{}^{35}ClF\cdots{}^{84}Kr$, $CH_2{}^{35}ClF\cdots{}^{86}Kr$, and $CH_2{}^{37}ClF\cdots{}^{84}Kr$) of the complex $CH_2ClF\cdots Kr$ display very similar inversion splittings, 0.628(2) MHz, due to the tunneling motions of Kr within two equivalent configurations. This splitting is about one-fifth of that measured for the homologue complex $CH_2ClF\cdots Ar$, 2.922 MHz.[11] From a model based on distributed polarizability calculations and adjusted to the experimental data, we propose a van der Waals potential energy surface and feasible pathways for these large amplitude internal motions. The dissociation energy (2.5 kJ/mol) was estimated slightly larger than that of the related complexes difluoromethane−Kr[9] (1.9 kJ/mol) and $CH_2ClF\cdots Ar$[11] (2.0 kJ/mol). The potential energy function does have the same typology as in the case of $CH_2ClF\cdots Ar$, that is, in a first approximation, the rare gas atom tunneling motion is a rotation around the C−Cl bond.[11] However, the lowest energy tunneling barrier for the motion of the Kr atom was estimated to be 74 cm^{-1}, slightly higher than that found for CH_2ClF−Ar[11] (61 cm^{-1}).

Acknowledgment. We thank Aldo Millemaggi for technical help. This work was supported by the University of Bologna, the Ministero dell'Università e della Ricerca Scientifica e Tecnologica.

Supporting Information Available: Table of rotational transition frequencies. This material is available free of charge via the Internet at http://pubs.acs.org.

References and Notes

(1) Klots, T. D.; Emilsson, T.; Ruoff, R. S.; Gutowsky, H. S. *J. Phys. Chem.* **1989**, *93*, 1255−1264.
(2) Klots, T. D.; Emilsson, T.; Gutowsky, H. S. *J. Chem. Phys*. **1992**, *97*, 5335−5340.
(3) Xu, Y.; Jäger, W. *J. Chem. Phys*. **1997**, *106*, 7968−7980.
(4) Velino, B.; Melandri, S.; Maris, A.; Favero P. G.; Caminati, W. *Mol. Phys.* **2000**, *98*, 1919−1924.
(5) Velino, B.; Millemaggi, A.; Caminati, W. *J. Mol. Spectrosc*. **2002**, *215*, 73−77.
(6) Blanco, S.; Melandri, S.; Maris, A.; Caminati, W.; Velino, B.; Kisiel, Z. *Phys. Chem. Chem. Phys.* **2003**, *5*, 1359−1364.
(7) Velino, B.; Melandri, S.; Caminati, W. *J. Phys. Chem. A* **2004**, *108*, 4224−4227.
(8) Maris, A.; Melandri, S.; Caminati, W.; Rossi, I. *Chem. Phys. Lett.* **2005**, *407*, 192−198.
(9) Melandri, S.; Favero, P. G.; Caminati, W.; Velino, B., *J. Chem. Phys*. **2005**, *122*, 134310−1−7.
(10) Caminati, W.; Melandri, S.; Maris, A.; Ottaviani, P. *Angew. Chem., Int. Ed. Engl.* **2006**, *45*, 2438−2442.
(11) Ottaviani, P.; Caminati, W.; Grabow, J.-U. *J. Chem. Phys*. **2006**, *125*, 194302−1−6.
(12) López, J. C.; Favero, P. G.; Dell'Erba, A.; Caminati, W. *Chem. Phys. Lett.* **2000**, *316*, 81−87.
(13) Grabow, J.-U.; Stahl, W. *Z. Naturforsch. A.* **1990**, *45*, 1043. Grabow, J.-U. Doctoral thesis, Christian-Albrechts-Universität zu Kiel, Kiel, 1992. Grabow, J.-U.; Stahl, W.; Dreizler, H. *Rev. Sci. Instrum.* **1996**, *67*, 4072−4084.
(14) Balle, T. J.; Flygare, W. H. *Rev. Sci. Instrum.* **1981**, *52*, 33−45.
(15) Caminati, W.; Millemaggi, A.; Alonso, J. L.; Lesarri, A.; López, J. C.; Mata, S. *Chem. Phys. Lett.* **2004**, *1*, 392, 1−6.
(16) Grabow, J.-U. Habilitationsschrift, Universität Hannover, Hannover 2004; http://www.pci.uni-hannover.de/~lgpca/spectroscopy/ftmw.
(17) Kisiel, Z.; Fowler, P. W.; Legon, A. C. *J. Chem. Phys*. **1991**, *95*, 2283−2291.
(18) Kisiel, Z. *J. Phys. Chem*. **1991**, *95*, 7605−7612.
(19) Kisiel, Z. "PROSPE − Programs for Rotational SPEctroscopy", available at http://info.ifpan.edu.pl/~kisiel/prospe.htm.
(20) Blanco, S.; Lesarri, A.; López, J. C.; Alonso, J. L.; Guarnieri, A. *J. Mol. Spectrosc.* **1995**, *174*, 397−416.
(21) One table of transition frequencies is available as Supporting Information.
(22) Pickett, H. M. *J. Chem. Phys.* **1972**, *56*, 1715−1723. Pickett, H. M. *J. Mol. Spectrosc.* **1991**, *148*, 371−377.
(23) Watson, J. K. G. In *Vibrational Spectra and Structure*; Durig, J. R., Ed.; Elsevier: New York/Amsterdam, 1977; Vol. 6, p 1.
(24) Kraitchman, J. *Am. J. Phys*. **1953**, *21*, 17−25.
(25) Costain, C. C. *Trans. Am. Crystallogr. Assoc*. **1966**, *2*, 157−164.
(26) Caminati, W.; Favero, P. G.; Melandri, S.; Meyer, R. *Chem. Phys. Lett.* **1997**, *268*, 393−400.
(27) Millen, D. J. *Can. J. Chem*. **1985**, *63*, 1477−1479.
(28) Read, W. G.; Campbell, E. J.; Hederson, J. *J. Chem. Phys*. **1983**, *78*, 3501−3508.
(29) Bettens, R. P. A.; Spycher, R. M.; Bauder, A. *Mol. Phys*. **1995**, *86*, 487−511.
(30) Meyer, R. *J. Mol. Spectrosc*. **1979**, *76*, 266−300.